

NANO MICRO  
**small**

Supporting Information

for *Small*, DOI: 10.1002/smll.201102179

Cobalt-Doping-Induced Synthesis of Ceria Nanodisks and  
Their Significantly Enhanced Catalytic Activity

*Xiao-Hui Guo,\* Chao-Chao Mao, Ji Zhang, Jun Huang, Wan-Nv Wang, Yong-Hui Deng, Yao-Yu Wang, Yong Cao, Wei-Xin Huang, and Shu-Hong Yu\**

## Supporting Information

### Cobalt Doping-Induced Synthesis of Ceria Nanodiscs and Their Significantly Enhanced Catalytic Activity\*\*

Xiao-Hui Guo<sup>\*</sup>, Chaochao Mao, Ji Zhang, Jun Huang, Wanv Wang, Yong-Hui Deng,  
Yao-Yu Wang, Yong Cao, Wei-Xin Huang, Shu-Hong Yu<sup>\*</sup>

#### Characterization

**Brunauer-Emmett-Teller (BET).** The specific surface area (SBET) was calculated by using adsorption data in a relative pressure range from 0.18 to 0.35. By using the Barrett-Joyner-Halenda (BJH) model, the pore volumes and pore size distributions were derived from the adsorption branches of isotherms, and the total pore volumes (Vt) were estimated from the adsorbed amount at a relative pressure  $P/P_0$  of 0.992. The BET surface area of catalyst was obtained from the adsorption and desorption N<sub>2</sub> isotherms that were collected on a Micromeritics Tri-Star 3000 instrument at 77 K. Prior to the measurements, all samples were degassed at 573 K until a stable vacuum of ca. 5 m Torr was reached.

**X-ray diffraction (XRD).** Powder X-ray diffraction data were obtained with a Bruker D8 diffractometer using Cu K $\alpha$  radiation ( $\lambda = 1.5406 \text{ \AA}$ ). The diffraction patterns were taken in the Bragg's angle ( $2\theta$ ) range from  $10^\circ$  to  $80^\circ$  at room temperature.

**Scanning electron microscope (SEM).** The particle morphologies were observed by using a FEI Quanta-400 FEG scanning electron microscope (FE-SEM) with accelerating voltage of 20 KV.

**Transmission electron microscope (TEM).** Transmission electron microscopy images were recorded on a JEOL-2100F electron microscope operating at 200 kV. Energy dispersion spectra (EDS) were obtained from an attached Oxford Link ISIS energy-dispersive spectrometer fixed on the JEM-2011 electron microscope.

**X-ray photoelectron spectroscopy (XPS).** XPS analysis was performed on ESCALAB 250 spectrometer using Mg K $\alpha$  radiation (1253.6 eV, pass energy of 20.0 eV). The carbonaceous C1 s line (284.6 eV) was used as the reference to calibrate the binding energies (BE).

**Raman spectroscopy.** Raman spectra were determined on a Renishaw (U.K.) spectrometer with

an Ar ion laser of 514.5 nm excitation wavelength.

**Electron paramagnetic resonance (EPR).** EPR spectra analysis was performed at JES-FA200 electronic spin resonance spectrophotometer.

**Diffuse reflectance (DR) UV - Vis.** DR UV-Vis spectra of the solids diluted in BaSO<sub>4</sub> were recorded at room temperature on a Shimadzu UV 2450 Spectrometer equipped with an integrating sphere and using BaSO<sub>4</sub> as reference.

**Catalytic activity measurement of ceria over CO oxidation.** The catalytic activity tests were performed at atmospheric pressure in a quartz tube micro reactor (i.d. 3 mm). The catalyst weight was 50 mg, and the total flow rate of the reaction gas was 37 ml /min, with a composition of 1% CO– 20% O<sub>2</sub> (balanced with He gas). Before reaction, the catalysts were pretreated with He (50 mL /min) at 373 K for 0.5 h. Reactions were carried out with a flux of 100 mL /min at 298 K in CO and O<sub>2</sub> and He as balance. Kinetic data were acquired after reaction for 60 min. The composition of the influent and effluent gas was detected with an online GC-17A gas chromatograph equipped with a TDX-01 column. The conversion of CO was calculated from the change in CO concentrations in the inlet and outlet gases.

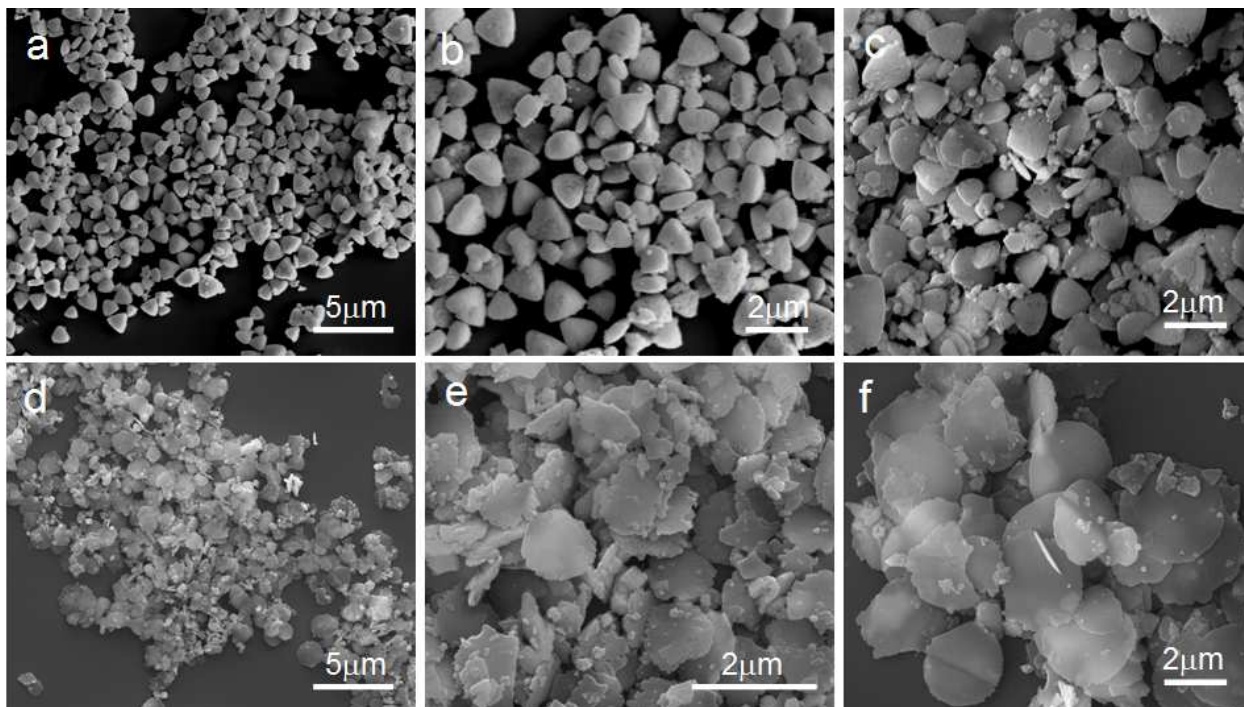


**Figure S1.** SEM images of the cerium hydroxide carbonate precursors prepared by varying the doping amount of cobalt nitrate. (a, b) 2 wt. %; (c) 5 wt. %; (d, e) 10 wt. %; (f) 20 wt. %. The hydrothermal reaction was carried out at 160 °C for 24 h.

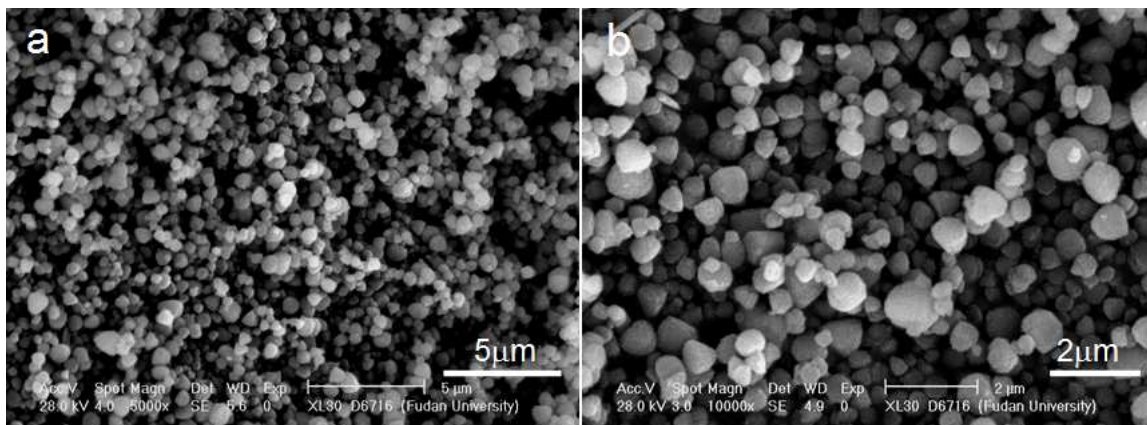


**Figure S2.** SEM images of the ceria sample prepared without cobalt doping by hydrothermal process at 160 °C for 24 h and followed by calcination at 550 °C for 6 h.

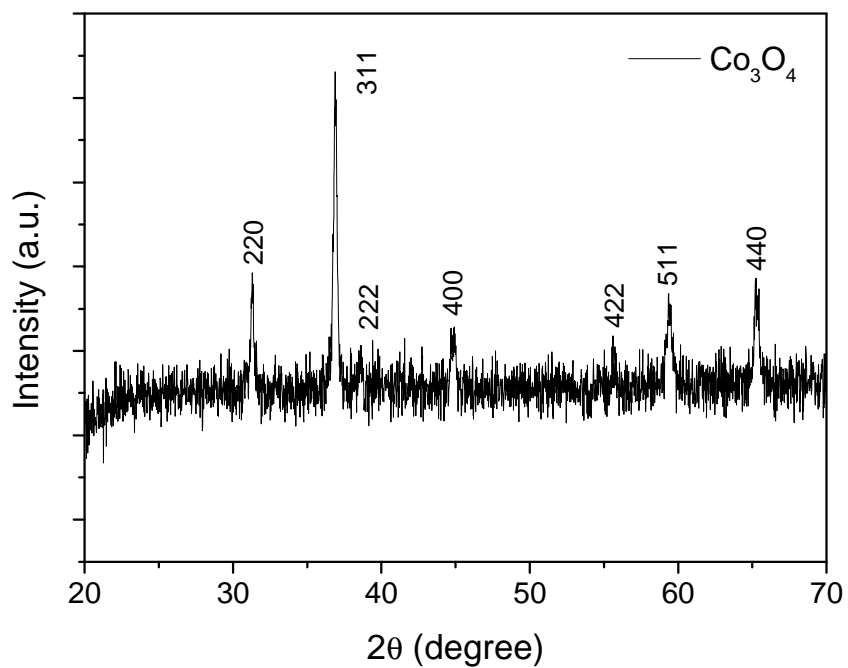


**Figure S3.** XRD pattern of the prepared porous  $\text{Co}_3\text{O}_4$  samples prepared by calcination of the cobalt carbonate precursor at 550 °C for 6 h.

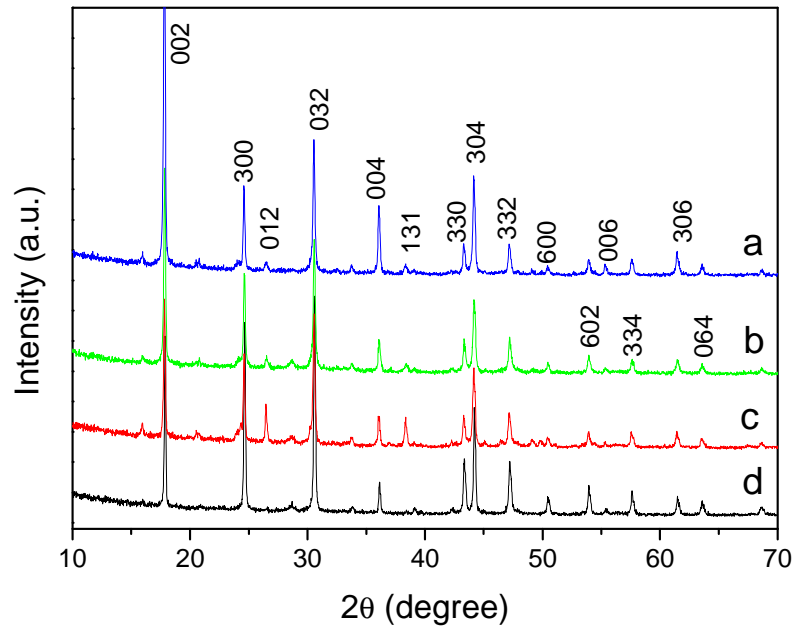


**Figure S4.** XRD patterns of the cerium hydroxide carbonate precursors prepared by hydrothermal process at 160 °C for 24 h, using different amount of cobalt nitrate. (a) 20 wt.%; (b) 10 wt.%; (c) 5 wt.%; (d) 2 wt.%.

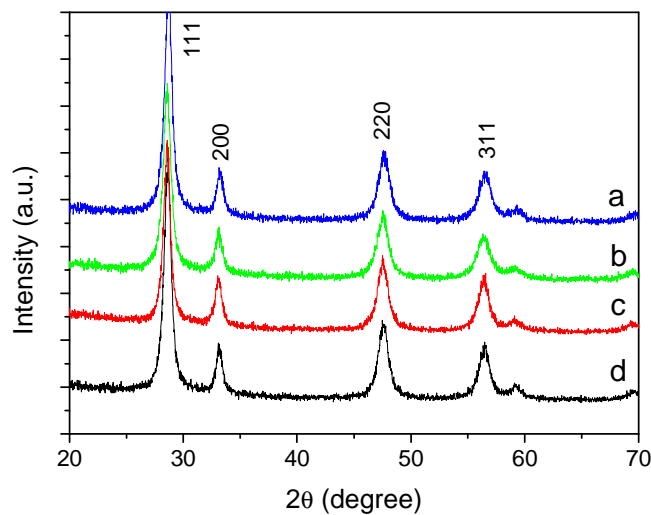


**Figure S5.** XRD patterns of the prepared ceria nanostructures prepared by hydrothermal process at 160 °C for 24 h, using different doping amount of cobalt nitrate. All samples were calcinated at 550 °C for 6 h. (a) 20 wt.%; (b) 10 wt.%; (c) 5 wt.%; (d) 2 wt.%.

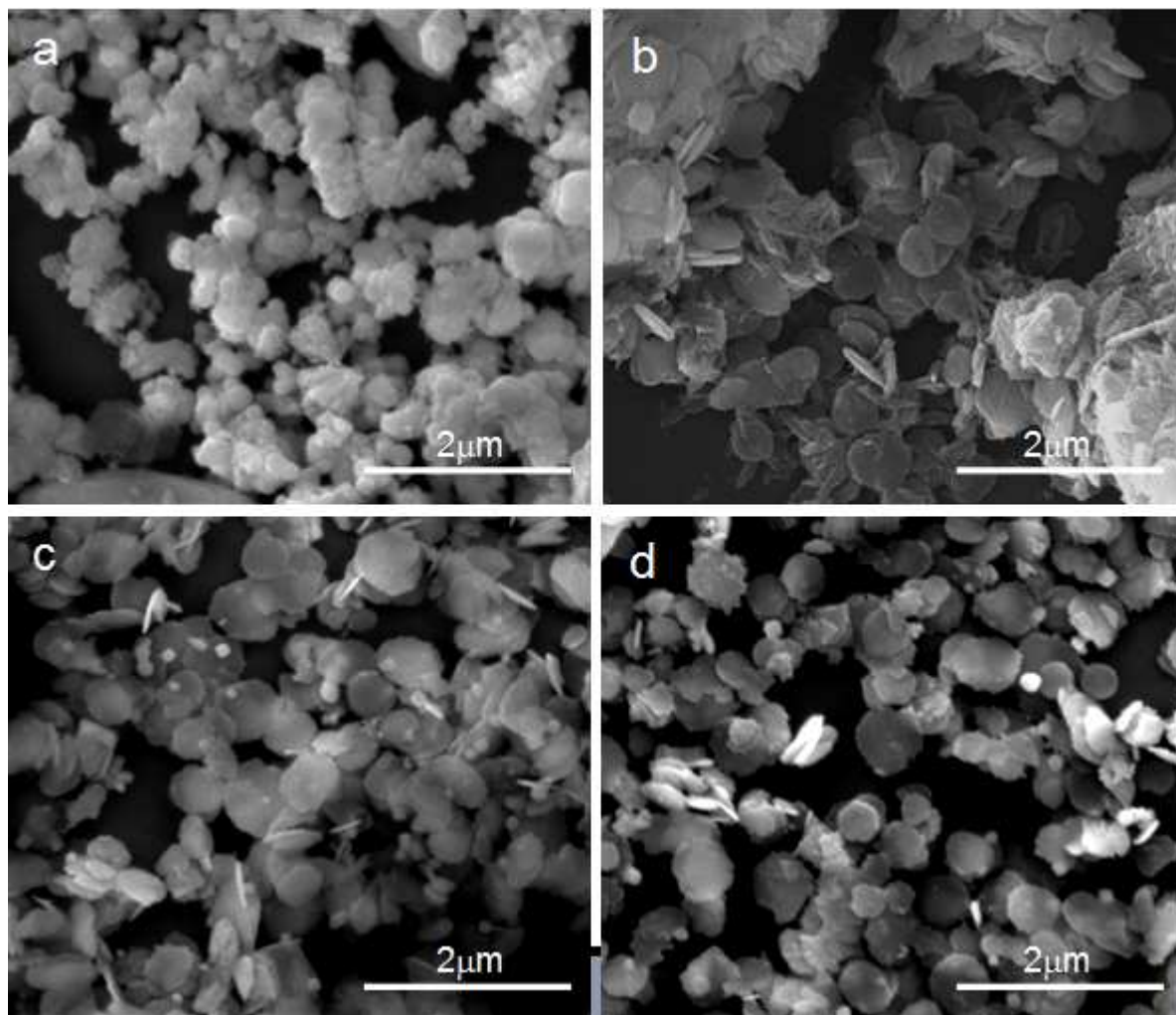


**Figure S6.** SEM images of the ceria samples prepared by hydrothermal process after reaction at 160 °C for different reaction time: (a) 2 h; (b) 4 h; (c) 8 h; (d) 12 h. The doping amount of cobalt nitrate was kept as 20 wt. %. All samples were calcinated at 550 °C for 6 h.

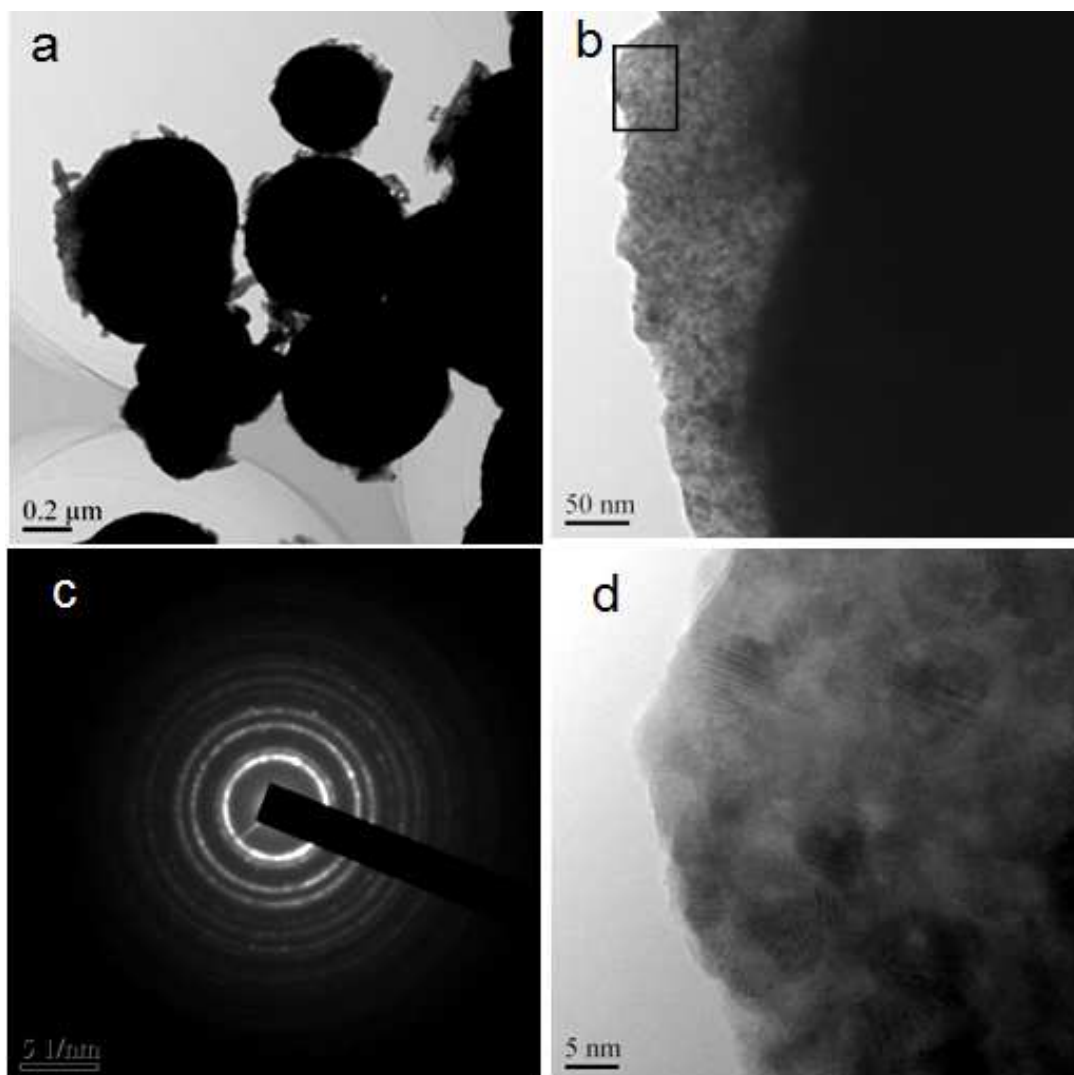


**Figure S7.** Structural analysis of the obtained ceria sample prepared by hydrothermal process after reaction at 160 °C for 2 h. The doping amount of cobalt nitrate was kept as 20 wt. %. The sample was calcinated at 550 °C for 6 h. (a) TEM image; (b) TEM image with magnification; (c) selected area electron diffraction pattern taken in the marked area in (b); (d) High resolution TEM image taken in the selected area marked in (b).



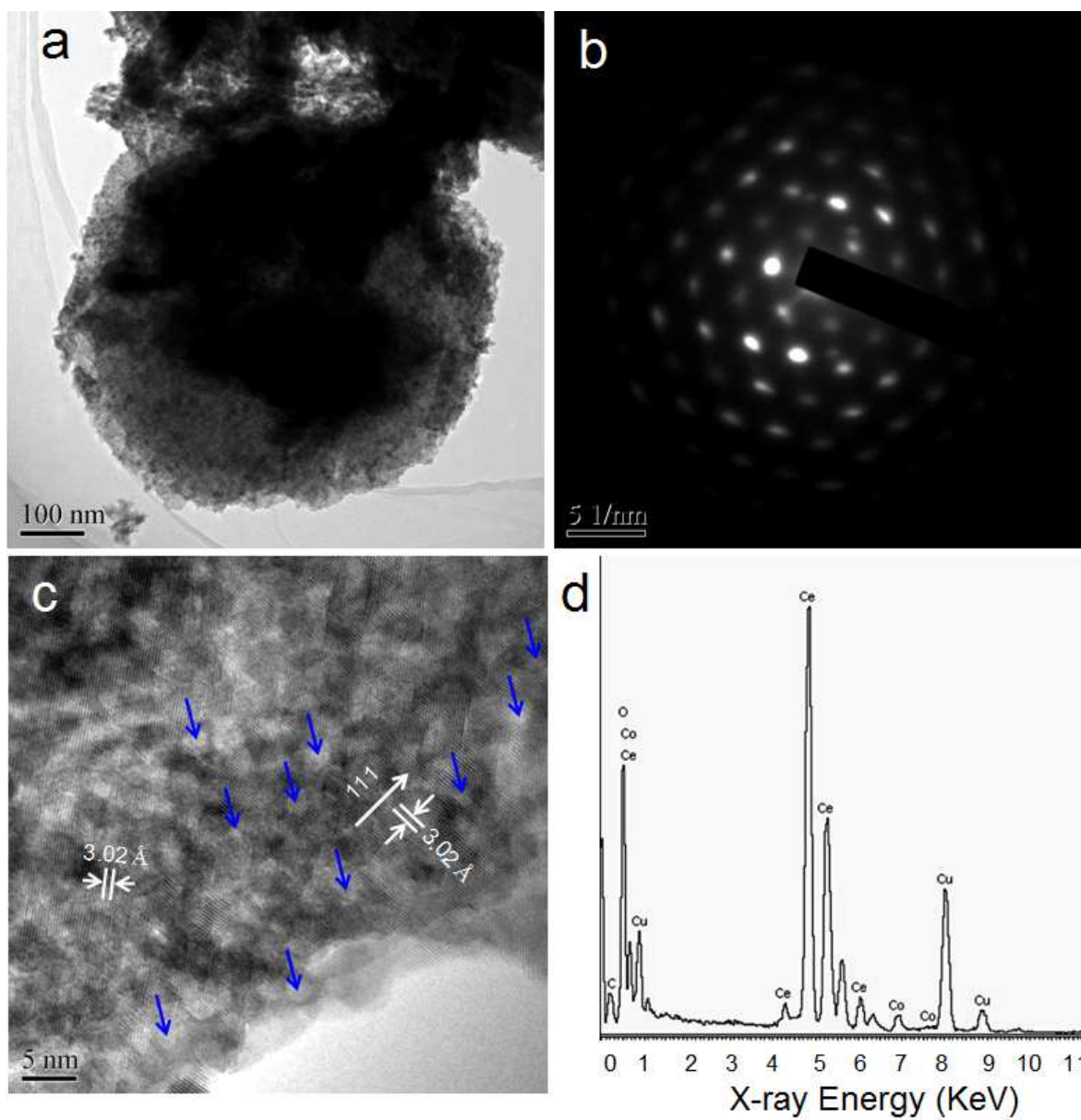


**Figure S8.** The structural and compositions analysis of the obtained ceria sample doped with 20 wt. % cobalt nitrate by hydrothermal process at 160 °C for 4 h. The arrows marked in (c) show the dislocations located in the ceria lattice. (d) Energy dispersion spectrum (EDS).



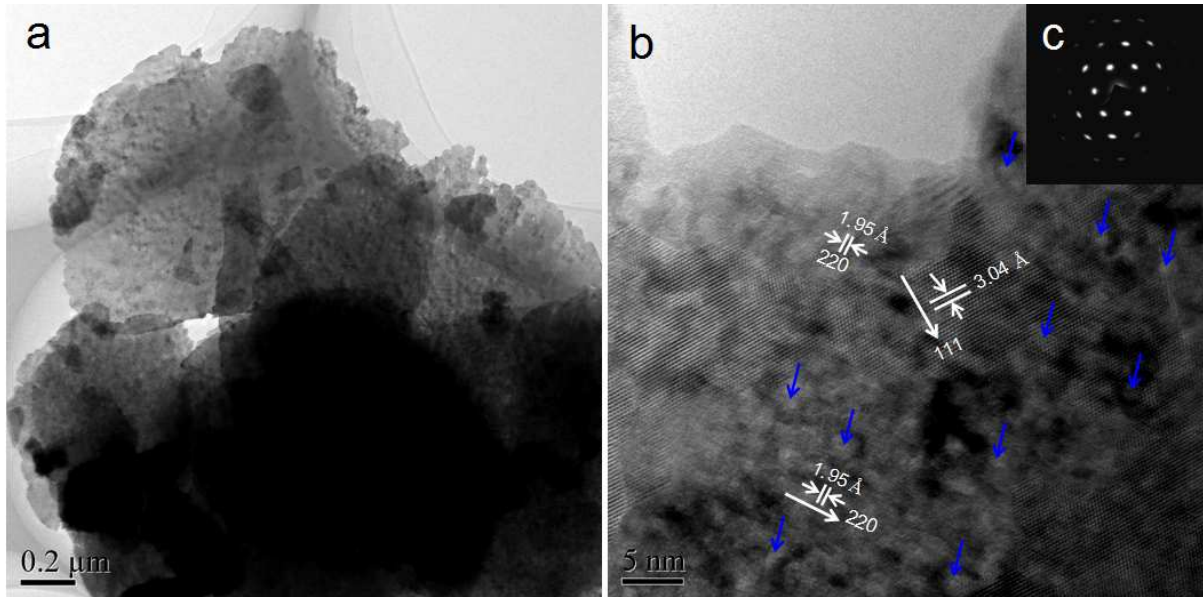


**Figure S9.** The structural analysis of the obtained ceria sample doped with 20 wt. % cobalt nitrate by hydrothermal process at 160 °C for 8 h. The arrows marked in (b) show the dislocations located in the ceria lattice. (c) Selected area diffraction pattern.

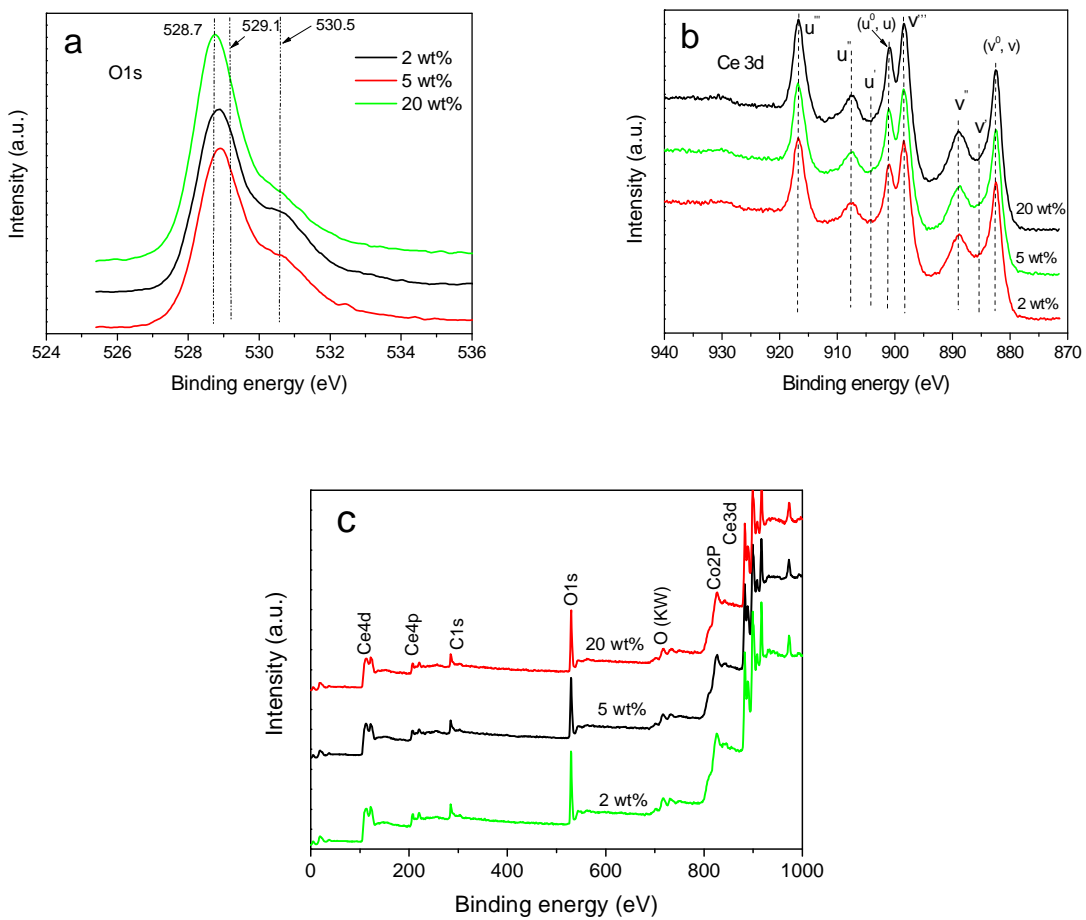


**Figure S10.** XPS spectra of the obtained ceria samples doped with different amounts of cobalt nitrate precursor: (a) O1s; (b) Ce3d; (c) survey XPS spectrum.

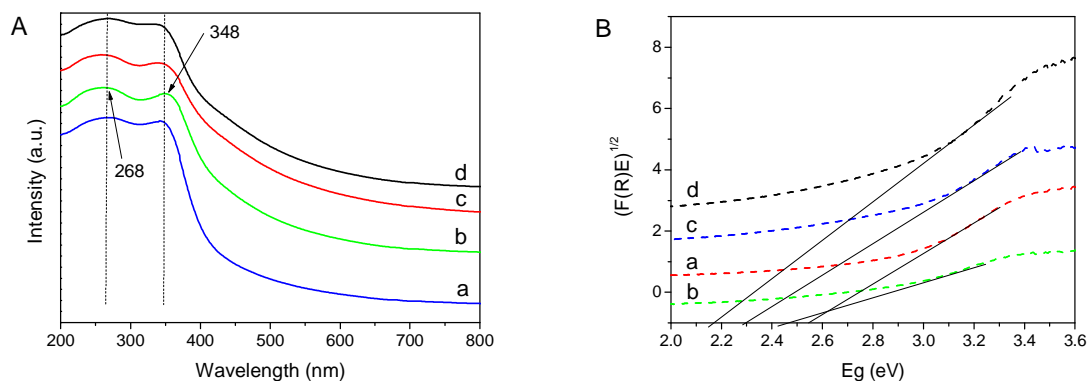


**Figure S11.** (A) DR UV-Vis spectra of the ceria samples prepared by doping different amount of cobalt nitrate. (B) Plots of  $\alpha(h\nu)^{1/2}$  vs photon energy ( $E_g$ ) for different ceria samples prepared by varying the doping amount of cobalt nitrate (wt. %). (a) 2; (b) 5; (c) 10; (d) 20.

The UV - Vis spectra of the obtained ceria displayed an intense absorption band with maximum at about 348 nm. According to the literature, the bands at 260 and 313 nm for pure  $\text{CeO}_2$  can be ascribed to the overlapping of the  $\text{Ce}^{4+} \leftarrow \text{O}^{2-}$  charge transfer and interband transitions, respectively.<sup>1</sup> the introduction of Co induced an obvious shift of the maximum towards higher wavelength. Namely, the UV - Vis spectra for the synthesized ceria have two bands at ca. 268 and 348 nm wavelength can be attributed to the  $\text{O}^{2-} \rightarrow \text{Ce}^{4+}$  and  $\text{O}^{2-} \rightarrow \text{Ce}^{3+}$  charge transfer (CT) transitions, respectively. This can be explained as an introduction of energy levels in the interbandgap, implying a decrease in the bandgap of the ceria material when doping with transition metal ions.<sup>2</sup>

1) A. Bensalem, J. C. Muller, F. Bozon-Verduraz, *J. Chem. Soc. Faraday Trans*, **1992**, 88, 153.

2) J. A. Navio, M.C. Hidalgo, G. Colon, S.G. Botta, M.I. Litter, *Langmuir*, **2001**, 17, 202.

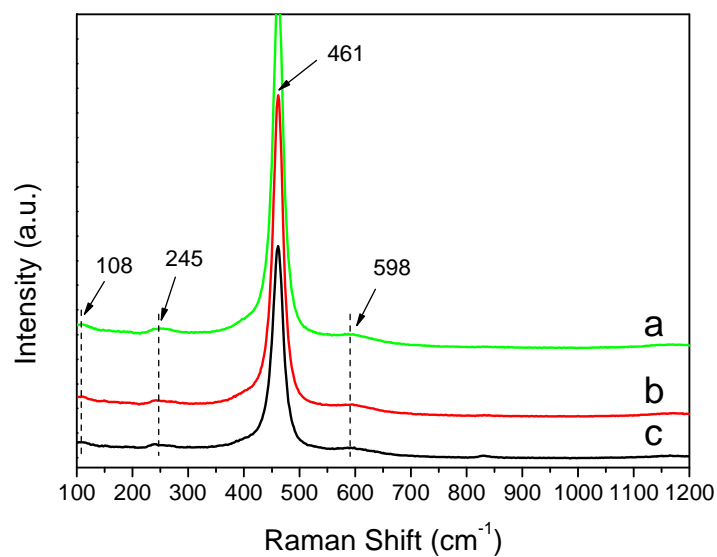


**Figure S12.** Raman spectra of the obtained ceria samples prepared by doping with different amount of cobalt nitrate precursor. (a) 20 wt.%; (b) 5 wt.%; (c) 2 wt.%.

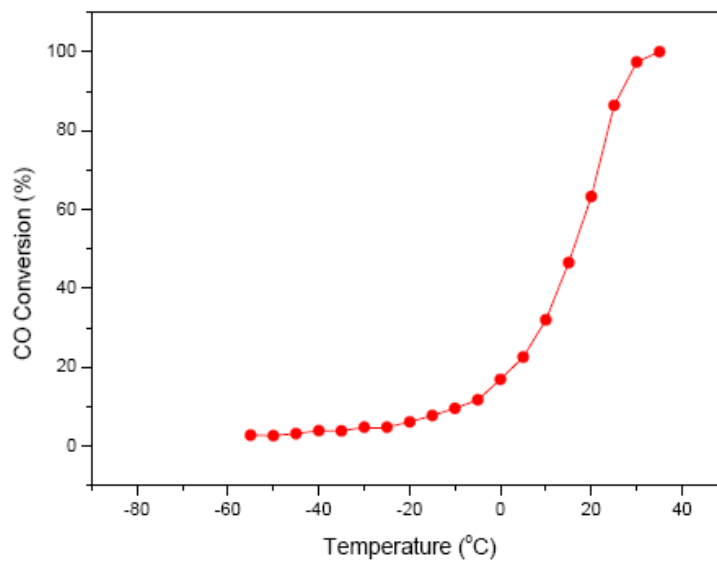


**Figure S13.** The light-off curve of CO oxidation over Au supported ceria catalyst at low-temperature, wherein, the obtained ceria sample loaded with Au (3 wt. %). The ceria sample prepared by hydrothermal process at 160 °C for 24 h, doping with 20 wt. % cobalt nitrate. The sample was calcinated at 550 °C for 6 h.

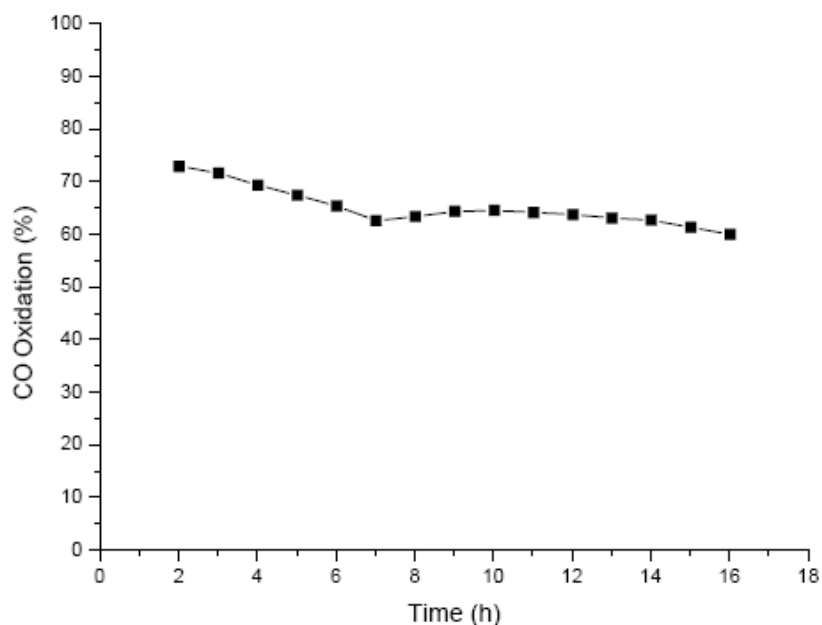


**Figure S14.** Catalytic reducibility curve of CO oxidation over Au supported on nanodisc ceria catalyst with reaction time at catalytic reaction temperature of  $\sim 25$  °C. The obtained ceria sample was loaded with Au (3 wt. %).

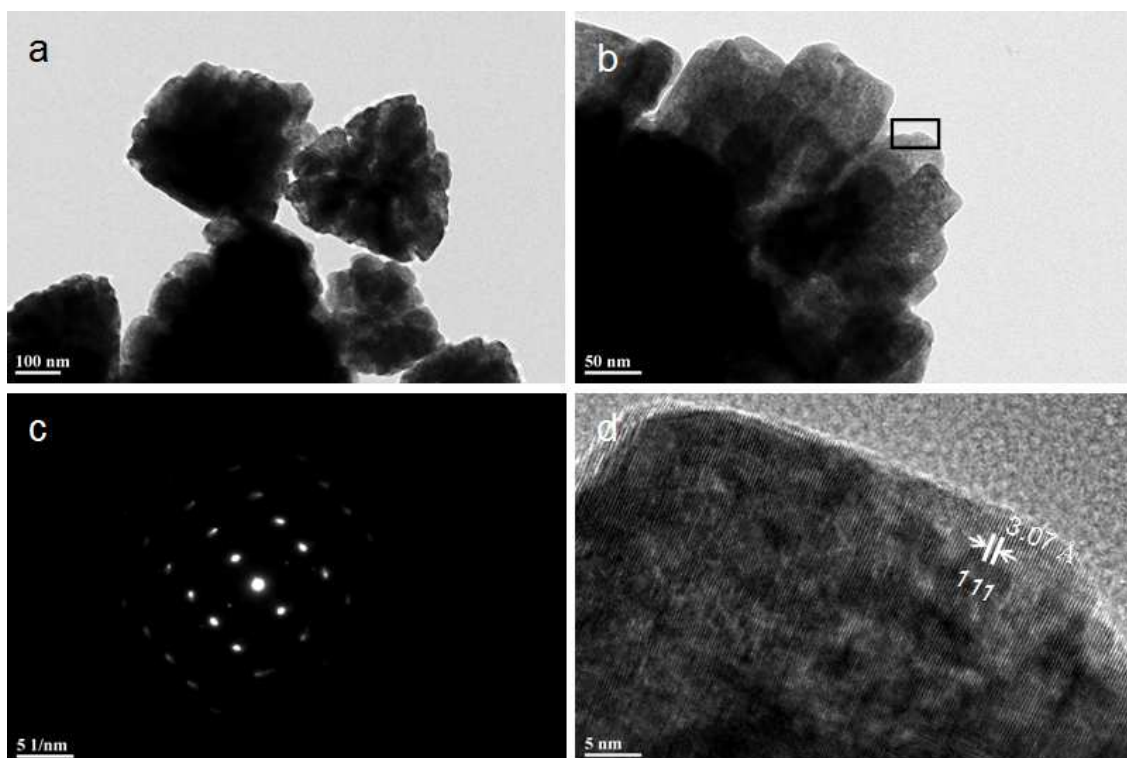


**Figure S15.** Structural analysis of the prepared ceria sample by hydrothermal process at  $160$  °C for 24 h, doping with 2 wt.% cobalt nitrate. (a,b) TEM images; (c) Selected area diffraction pattern taken in marked area shown in (b); (d) High resolution TEM image taken in the area marked in (b).

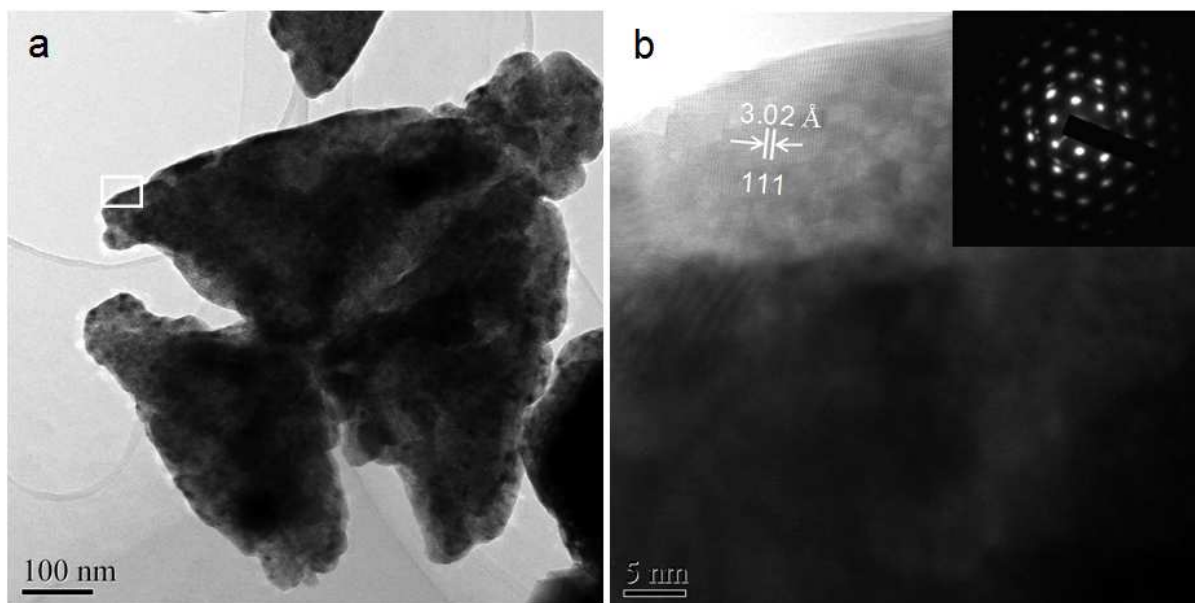


**Figure S16.** Structural analysis of the prepared ceria sample by hydrothermal process at 160 °C for 24 h, doping with 5 wt.% cobalt nitrate. (a) TEM images; (b) High resolution TEM image taken in the area marked in (b). Inset shows selected area diffraction pattern taken in marked area shown in (a).

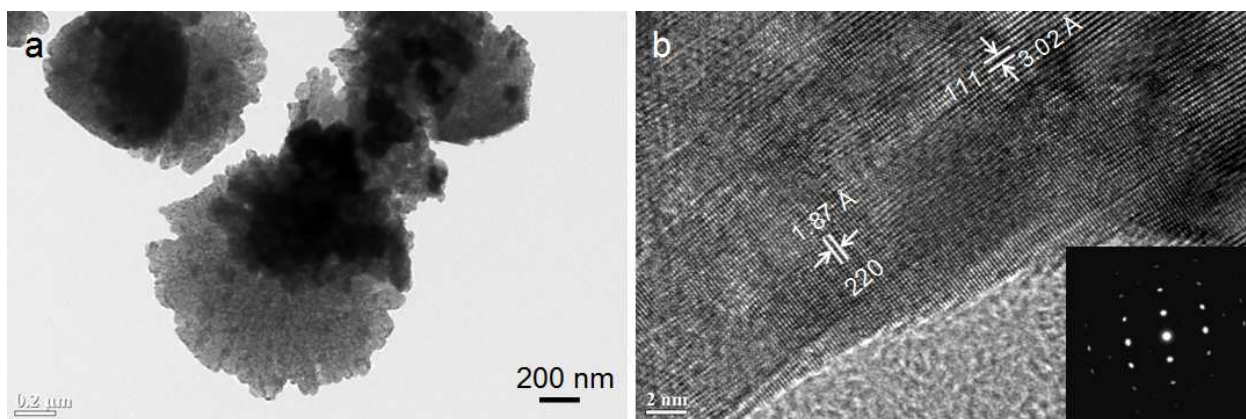


**Figure S17.** Structural analysis of the prepared ceria sample by hydrothermal process at 160 °C for 24 h, doping with 10 wt.% cobalt nitrate. (a) TEM images; (b) High resolution TEM image taken in the area marked in (b). Inset shows selected area diffraction pattern taken in marked area shown in (a).

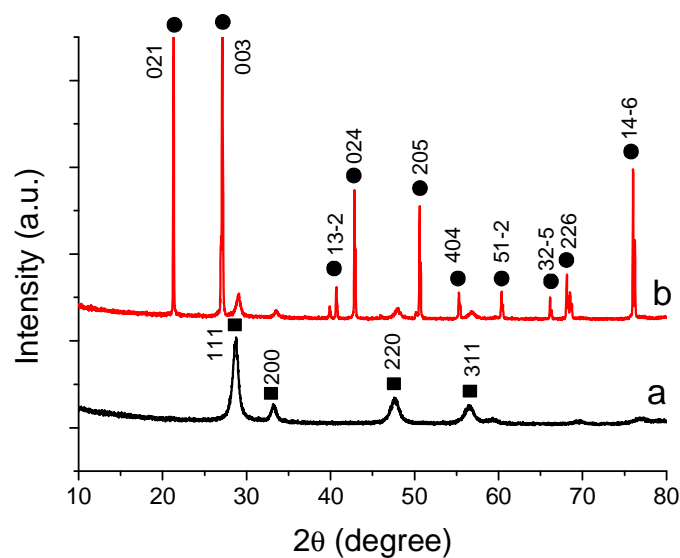


**Figure S18.** XRD patterns of the ceria catalysts prepared by doping with 20 wt. % cobalt nitrate after (a) and before (b) catalytic reaction. ● denotes  $\text{Ce}_7\text{O}_{12}$  phase, ■ denotes cubic phase of ceria.

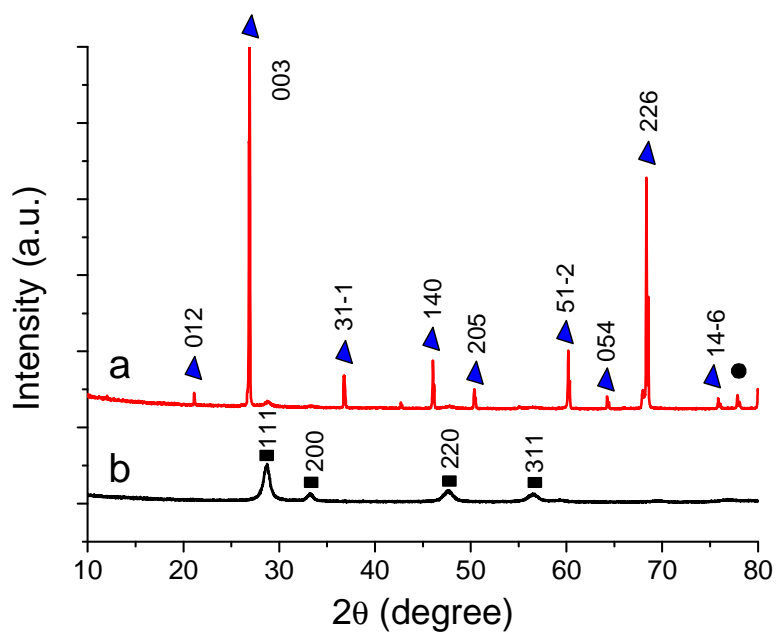


**Figure S19.** XRD patterns of the cobalt doped ceria catalyst loading 3 wt. % Au. The ceria sample was prepared by doping with 20 wt. % cobalt nitrate. (a) after catalytic reaction; (b) before catalytic reaction. ▲ denotes  $\text{Ce}_7\text{O}_{12}$  phase, ■ denotes cubic phase of ceria, and ● denotes Au phase.